 doi:10.20944/preprints202106.0546.v1

Article

Refraction of oblique shock wave on a tangential discontinuity

Pavel Bulat [1,*], Anzhelika Melnikova [1], Vladimir Upyrev [1] and Konstantin Volkov [2]

[1] BSTU «VOENMEH» named after D.F. Ustinov; pavelbulat@mail.ru
[2] Kingston University; k.volkov@kingston.ac.uk
* Correspondence: pavelbulat@mail.ru

Abstract: Refraction of an oblique shock wave on a tangential discontinuity dividing two gas flows with different properties is considered. It is shown that its partial reflection occurs excepting of geometrical diffraction of an oblique shock. Another oblique shock, expansion wave or weak discontinuity that coincides with Mach line, can act as a reflected disturbance. This study focuses on relationships which define the type of reflected discontinuity and its parameters. Domains of existence of various shock-wave structures with reflected disturbances of two types and boundaries between them are defined. The domains of parameters with one or two solutions exist for the characteristic refraction. Conditions of the regular refraction and the Mach refraction are formulated, and boundaries between those two refraction types are defined for various types of gases. Refraction phenomena in various engineering problems (hydrocarbon gaseous fuel and its combustion products, diatomic gas, fuel mixture of oxygen and hydrogen etc.) are discussed.

Keywords: shock wave process; shock-wave structure; refraction; domain of existence

1. Introduction

The processes of transformation of a gas-dynamic system with parameters f_1 into a system with parameters f_2 are called shock-wave processes, where f_1 and f_2 are some gas-dynamic variables before and behind the gas dynamic discontinuity.

Gas-dynamic waves and discontinuities can be divided into two large groups. The first group includes normal waves and discontinuities through which the gas flows, and they are referred to as shock wave processes. The second group includes contact and tangential discontinuities, through the surfaces of which the gas does not flow, and they cannot be considered as shock wave process. A tangential discontinuity is also called a sliding line because it can separate flows of various gases with different densities, velocities and temperatures. The static pressure on opposite sides of the tangential discontinuity is always the same. The tangential discontinuity is usually denoted by the symbol τ. It appears in shock-wave structures formed as a result of the interaction of shock waves with each other and with solid walls. The reason for the formation of tangential discontinuity lies in the fact that at different shock waves, included in the shock-wave structures, the value of the total pressure loss and, accordingly, the flow rate is different.

The theory of gas-dynamic discontinuities consists of two large sections, the theory of interference (intersections, interactions) of discontinuities and waves with each other, and the theory of their refraction (refraction) on contact and tangential discontinuities [1]. Contact and tangential discontinuities cannot intersect with each other.

The problem of refraction of an oblique shock wave on a tangential discontinuity is consistently presented in [2]. There are cases of regular refraction (RRefr) [3] and Mach (irregular) refraction (MRefr) [4]. In the first case, the flow is everywhere supersonic. In the second case, there are regions where the Mach number is less than unity (M<1).

The theory of regular refraction is developed in [5]. A number of studies are devoted to the experimental research of both regular and irregular refraction [6–8]. An attempt to systematize the flow patterns arising during refraction, both regular and Mach, is made in [4, 9]. A similar problem is solved in a non-stationary formulation in [10].

The interaction of an oblique shock wave with the interface between the media leads to the development of complex non-stationary shock-wave configurations [6–8, 11]. The passage of a shock wave through a medium containing gas bubbles or liquid droplets leads to curvature of the wave front, shock waves interaction, and the development of multiple vortices.

A theoretical analysis of the emerging shock-wave configurations using shock poles is given in [12]. The boundaries of the regions of existence of refraction modes with a rarefaction wave and the region of existence of refraction with a reflected shock wave with a change in the angle of inclination of the contact discontinuity are determined. The generation of vorticity and the evolution of vortex structures are discussed, as well as the grid convergence of the solution [13]. An exact solution to the problem of refraction of a plane shock wave at a contact discontinuity (regular case) is given, and the suppression of the Richtmyer–Meshkov instability upon application of a magnetic field is discussed in [14, 15]. Exact solutions of the problem are given in both one-dimensional and two-dimensional cases of regular refraction of a shock wave at a contact discontinuity.

Various modes of shock wave refraction using experimental and numerical methods are studied in [3]. Numerical calculations are carried out on the basis of a TVD scheme of the 2nd order of accuracy and an approximate method for solving the Riemann problem. The calculated data are in good agreement with the results of measurements and the results of theoretical analysis, with the exception of the high Mach numbers of the incident shock wave.

Two-dimensional calculations based on the Godunov-type scheme of the second order of accuracy are carried out in [16]. The density discontinuity is oriented at an angle of 75 degrees to the horizontal, and the Mach number of the shock wave is 1.2. The MUSCL scheme is used in [17] to calculate the flow structure at different angles of inclination of the discontinuity. Various difference schemes are compared in [18].

A numerical study of the Richtmyer–Meshkov instability in the interaction of a strong shock wave with a discontinuity in the density of a rectilinear and sinusoidal shape is carried out in [19]. The refraction of a shock wave upon its interaction with a near-wall layer of a heated gas is investigated in [20]. A wide range of issues related to the interaction of shock waves with contact discontinuities and the formation of the Richtmyer–Meshkov instability are discussed in [21]. The refraction of a spherical shock wave at the air – water interface is considered in [22]. The results of calculations using the through-counting scheme and using the level function method are compared, which makes it possible to single out the contact gap and trace its evolution over time. The application of discontinuity detection schemes as applied to the refraction of shock waves at the interfaces between media is discussed in [23, 24].

Although, many theoretical, experimental and computational studies have been published for past years [25–31], research of different types of refraction is far from complete. In this study, domains of existence of various shock-wave structures with reflected disturbances of two types and boundaries between them are defined. Conditions of the regular refraction and the Mach refraction are formulated, and boundaries between those two refraction types are defined for various types of gases. Refraction phenomena in various engineering problems (hydrocarbon gaseous fuel and its combustion products, diatomic gas, fuel mixture of oxygen and hydrogen etc.) are discussed.

2. Regular refraction

The scheme of regular refraction is shown in Figure 1, where σ_1 is the incident shock wave, σ_2 is the refracted shock wave, ω_3 is the reflected rarefaction wave, σ_3 is the reflected shock wave, ν_3 is the reflected weak discontinuity, τ is the tangential discontinuity, $\leftarrow$ is the left discontinuity, $\rightarrow$ is the right discontinuity, T is the refraction point. The subscript + denotes the flow quantities in original flow above τ, and subscript – denotes the flow quantities in the original flow under τ.

Preprints (www.preprints.org) | NOT PEER-REVIEWED | Posted: 22 June 2021 doi:10.20944/preprints202106.0546.v1

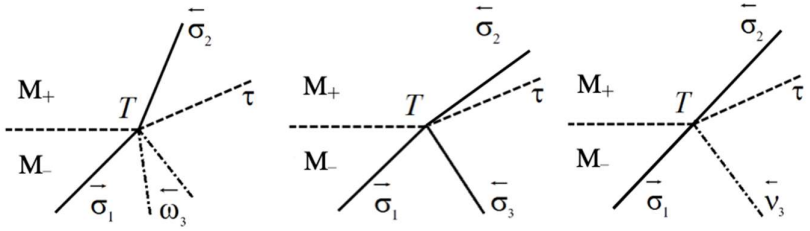

(**a**) (**b**) (**c**)

Figure 1. Regular refraction of oblique shock wave σ_1 on tangential discontinuity τ: (a) refraction with reflected rarefaction wave, (b) refraction with reflected shock wave, (c) characteristic refraction, where the reflected discontinuity is the discontinuous characteristic.

Refraction of the shock wave σ_1 on the tangential discontinuity leads to increasing (Figure 1a) or decreasing (Figure 1b) of its inclination angle. In the particular case, when the reflected discontinuity is a discontinuous characteristic, only the curvature of the incident shock wave changes. This refraction is called characteristic.

The equation of regular refraction is written as

$$\vec{\sigma}_1 + \tau \rightarrow \begin{cases} \vec{\omega}_3 + \tau + \vec{\sigma}_2, \\ \vec{\sigma}_3 + \tau + \vec{\sigma}_2, \\ \vec{\sigma}_2 + \tau. \end{cases} \tag{1}$$

The first equation corresponds to refraction with reflected rarefaction wave (Figure 1a), the second equation corresponds to refraction with reflected shock wave (Figure 1b), and the third equation corresponds to characteristic refraction (Figure 1c). Three types of regular refraction on shock polar are presented in Figure 2.

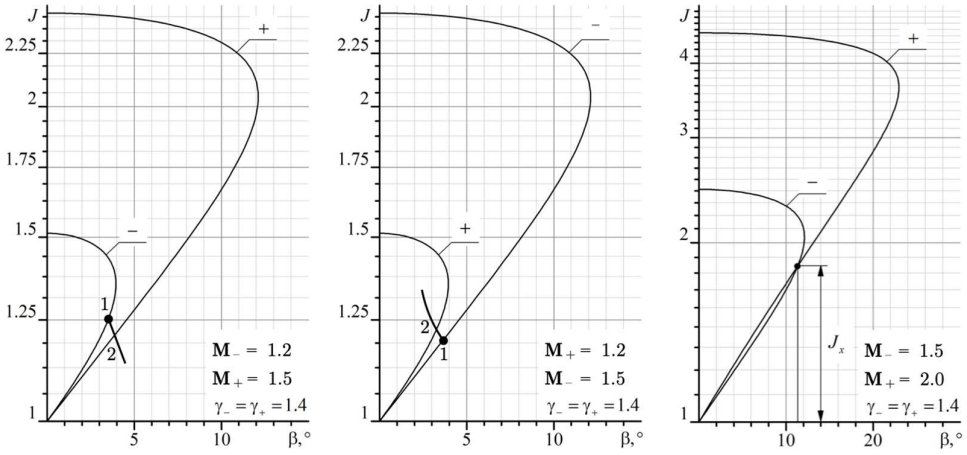

(**a**) (**b**) (**c**)

Figure 2. Three types of regular refraction on shock polar: (a) refraction with reflected rarefaction wave, (b) refraction with reflected shock wave, (c) characteristic refraction.

To solve equation (1), the conditions of dynamic compatibility are used, written in the form of equality of pressures p and inclination angles of the velocity vector at the tangential discontinuity behind the point T. These conditions are written as

$$\begin{cases} \vartheta_3 = \vartheta_2, \\ p_3 = p_2. \end{cases} \tag{2}$$

Preprints (www.preprints.org) | NOT PEER-REVIEWED | Posted: 22 June 2021 doi:10.20944/preprints202106.0546.v1

Subscript 2 denotes flow quantities behind the refracted shock wave, and subscript 3 denotes flow quantities behind the reflected discontinuity (Figure 1).

A partial case of regular refraction is characteristic refraction (Figure 1c), when the polar - and polar + intersect each other (Figure 2c). Since the reflected discontinuity is a discontinuous characteristic (weak discontinuity of the second order), the slope of the shock σ_1 does not change. Then, the conditions of dynamic compatibility on τ are written in the form of equality of the angles of flow turn

$$\beta_\sigma(\gamma_-, M_-, J_c) = \beta_\sigma(\gamma_+, M_+, J). \tag{3}$$

The flow turn angle at the shock is expressed by the formula

$$\beta_\sigma = \arctan\left(\sqrt{\frac{J_m - J}{J+\varepsilon}\frac{(1+\varepsilon)(J-1)}{J_m+\varepsilon+(1-\varepsilon)(J+1)}}\right) \tag{4}$$

Here, γ is the ratio of specific heat capacities at constant pressure and constant volume, and $\varepsilon = (\gamma-1)/(\gamma+1)$. The maximum intensity of the shock wave is $J_m = (1+\varepsilon)M^2-\varepsilon$.

For the case when a reflected discontinuity is a shock wave, an equation similar to equation (3) is written in the form

$$\beta_\sigma\left(\gamma_-, M_-, J_1\right) - \beta_\sigma\left(\gamma_-, \hat{M}_1, J_2 / J_1\right) = \beta_\sigma\left(\gamma_+, M_+, J_2\right) \tag{5}$$

Subscripts 1 and 2 denote relevant shock waves (Figure 1b) and flow quantities behind them, and subscript ^ denotes the flow quantities behind shock wave.

The Mach number behind the incident shock in equation (5) is found from the relation

$$\hat{M}_1 = \sqrt{\frac{M_-^2 - (1-E)(J_1+1)}{EJ_1}}, E = (1+\varepsilon J_1)(J_1+\varepsilon) \tag{6}$$

For the cases shown in Figures 1a and 2a, when the reflected discontinuity is a rarefaction wave, the conditions of dynamic compatibility take the form

$$\begin{aligned} &\beta_\sigma\left(\gamma_-, M_-, J_1\right) - \beta_\sigma\left(\gamma_-, \hat{M}_1, J_2 / J_1\right) = \beta_\sigma\left(\gamma_+, M_+, J_2\right), \\ &\beta_\omega = \omega(M_\omega) - \omega(M), M_\omega = \sqrt{\left(\left(1+\varepsilon\left(M^2-1\right)\right)J^{-\frac{2\varepsilon}{1+\varepsilon}} - 1 + \varepsilon\right)/\varepsilon}, \\ &\omega(M) = \arctan\left(\sqrt{\varepsilon\left(M^2-1\right)}\right) - \arctan\left(\sqrt{M^2-1}\right). \end{aligned} \tag{7}$$

In equation (7) for M_ω, J_2/J_1 is substituted instead J, and $\hat{M}_1$ is substituted instead M. Then, Prandtl-Mayer function $\omega(M)$ is found for M_ω and $\hat{M}_1$.

3. Characteristic refraction

In different technical problems, where there is refraction on the mixing layer or the interface between two media, different types of reflected discontinuities are preferable. So, with a reflected shock wave, the initial shock is enhanced, which is good for supersonic air intakes and wave compressors, but not good in cases where a shock wave attenuation is required [32, 33]. If it is required to protect a certain device from the impact of a shock wave, then refraction with a reflected rarefaction wave is preferable. Characteristic refraction separates these two cases.

The characteristic refraction corresponds to the intersection of shock polar $J(M_+)$ and shock polar $J(M_-)$, which is realized at a strictly defined intensity of the initial oblique

Preprints (www.preprints.org) | NOT PEER-REVIEWED | Posted: 22 June 2021 doi:10.20944/preprints202106.0546.v1

jump $J_c = J_c(M_+,M_-,\gamma_+,\gamma_-)$ at which equation (3) is satisfied. The condition for the equality of the intensities of the shocks $J_c(M_+,\gamma_+) = J_c(M_-,\gamma_-)$ reduces to the cubic equation

$$\sum_{n=0}^{3} A_i z^n = 0 \tag{8}$$

where

$$z = J_c - 1$$

$$A_3 = \frac{\gamma_+ M_+^2}{1+\varepsilon} - \frac{\gamma M_-^2}{1+\varepsilon_1}$$

$$A_2 = (\gamma_- - \gamma_+) M_-^2 M_+^2 - (M_+^2 - M_-^2) + \left[2\left(\frac{1}{1+\varepsilon_-} + \frac{1}{1+\varepsilon_+} \right) - \frac{\gamma_+ M_+^2 + \gamma_- M_-^2}{(1+\varepsilon_-)(1+\varepsilon_+)} \right] (\gamma_+ M_+^2 - \gamma_- M_-^2)$$

$$\Gamma_- = \frac{\gamma_- M_-^2}{\sqrt{M_-^2 - 1}}$$

$$\Gamma_+ = \frac{\gamma_+ M_+^2}{\sqrt{M_+^2 - 1}}$$

$$A_0 = (M_-^2 - 1)(M_+^2 - 1)(\Gamma_+^2 - \Gamma_-^2)$$

$$A_1 = 2(\gamma_+ M_+^2 - \gamma_- M_-^2)$$

$$\left[1 - \left(\frac{1}{1+\varepsilon_-} + \frac{1}{1+\varepsilon_+} \right) (\gamma_- M_-^2 + \gamma_+ M_+^2) + M_-^2 M_+^2 \left[\frac{\gamma_+ M_+^2}{1-\varepsilon_+} - \frac{\gamma_- M_-^2}{1-\varepsilon_-} + 2(\gamma_- - \gamma_+) \right] \right]$$

If the same gas flows on both sides of τ, then $\gamma_+ = \gamma_-$, $\varepsilon_+ = \varepsilon_-$, $\Gamma_+ = \Gamma_-$, and equation (8) is simplified

$$\begin{aligned}
A_3 &= \gamma(\gamma+1)(M_+^2 - M_-^2); \\
A_2 &= \gamma\left(\frac{\gamma+1}{2}\right)^2 (M_+^2 - M_-^2)\left[M_+^2 - M_-^2 - 4 - \frac{2\gamma+1}{(\gamma+1)^2} \right]; \\
A_1 &= \gamma^3 (M_+^2 - M_-^2)\left[4 - (\gamma+1)(M_+^2 M_-^2 - 2M_+^2 - M_-^2) \right]; \\
A_0 &= 2\gamma^4 (M_+^2 - M_-^2)(M_+^2 M_-^2 - M_+^2 - M_-^2).
\end{aligned} \tag{9}$$

Substituting (9) into (8) and excluding the solution $z = -(1-\varepsilon)$ that has no physical meaning, the unique solution is

$$J_c = 1 + \frac{1}{2}\left[\frac{M_+^2 + M_-^2}{1-\varepsilon} - 2 - \sqrt{\left(\frac{M_+^2 + M_-^2}{1-\varepsilon} \right)^2 - 4\gamma(M_-^2 M_+^2 - M_-^2 - M_+^2)} \right] \tag{10}$$

The equation (10) determines the intensity of the inlet shock, at which the characteristic refraction is realized, provided that the same gases flow on both sides of the tangential discontinuity.

The case when the same gases flow on both sides of τ, for example, air with $\gamma = 1.4$ is considered. An important conclusion follows directly from equation (10) that characteristic refraction is possible if

$$M_+ > \frac{M_-}{\sqrt{M_-^2 - 1}} \tag{11}$$

Preprints (www.preprints.org) | NOT PEER-REVIEWED | Posted: 22 June 2021 doi:10.20944/preprints202106.0546.v1

Formula (11) is interpreted in such a way that the shock polars do not intersect if $M<2^{1/2}$, since one of them lies completely inside the other (Figure 3).

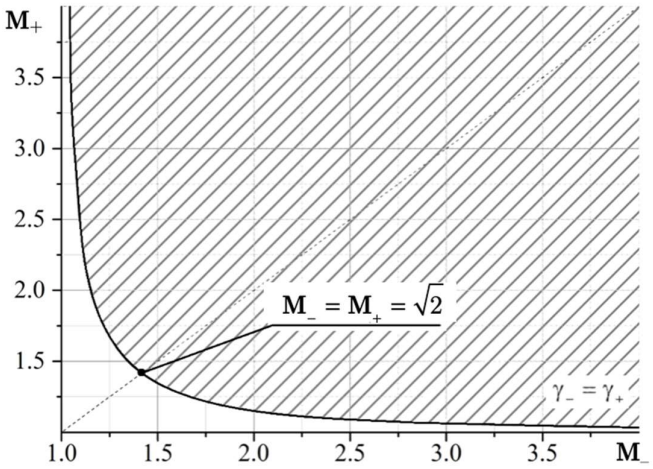

Figure 3. Domain of existence of characteristic refraction in air (the shaded area).

Equation (11) follows from the condition $J>1$, but on the other hand, the condition $J<J_m$ must also be satisfied. Then both shocks, the original shock σ_1 and the refracted shock σ_2, must be straight lines. Therefore, the second condition is that curves corresponding to characteristic refraction have an envelope

$$J_m\left(\gamma, M_+\right)=\frac{2\gamma}{\gamma+1}M_+^2-\frac{\gamma-1}{\gamma+1} \tag{12}$$

It corresponds to $M_- = \infty$. Solutions of equation (10) with limitations (11) and (12) are shown in Figure 4.

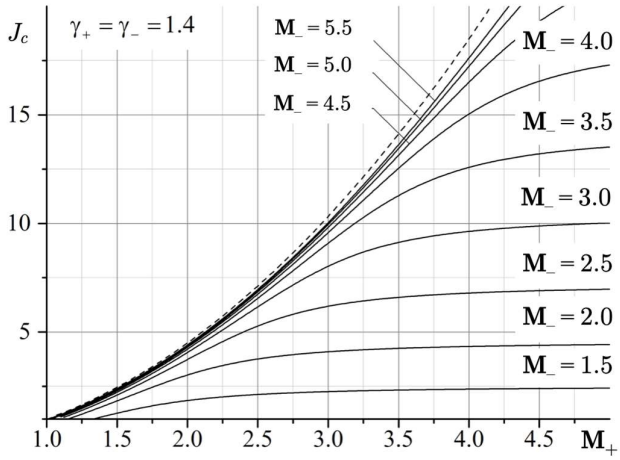

Figure 4. The values of the intensity J_c of the incident shock for characteristic refraction. The dashed line shows the envelope corresponding to the case when the refracted shock has the maximum intensity $J_2 = J_m$.

In the general case, when $\gamma_+ \neq \gamma_-$, it is necessary to solve the cubic equation (8). Unlike the previous case, the solution can have from one to three roots. Since $z \geq 0$, it follows from (8) that when one of the roots is equal to zero ($z=0$), the polars $J(\gamma_-, M_-)$ and $J(\gamma_+, M_+)$ have

Preprints (www.preprints.org) | NOT PEER-REVIEWED | Posted: 22 June 2021 doi:10.20944/preprints202106.0546.v1

the same derivatives at the origin ($\Gamma_- = \Gamma_+$), since $A_0 = 0$. From the equality $\Gamma_- = \Gamma_+$ it follows that between the numbers M_- and M_+ there must be a relation

$$M_+^2 = \frac{\Gamma_-^2}{2\gamma_+^2}\left[1 \pm \sqrt{1 - \frac{2\gamma_-^2}{\Gamma_-^2}}\right]. \quad (13)$$

The discriminant of equation (13) exists if $\gamma_+ \geq \gamma_-$. Therefore

$$M_- \geq 2\frac{\gamma_+^2}{\gamma_-^2}\left(1 + \sqrt{1 - \frac{\gamma_-^2}{\gamma_+^2}}\right), \quad (14)$$

or

$$M_- \leq 2\frac{\gamma_+^2}{\gamma_-^2}\left(1 - \sqrt{1 - \frac{\gamma_-^2}{\gamma_+^2}}\right). \quad (15)$$

Equations (14) and (15) determine the region of existence of characteristic refraction. The other two roots are obtained by solving the quadratic equation

$$A_3^0 z + A_2^0 z + A_1^0 = 0. \quad (16)$$

In equation (16), the coefficients A are calculated by formulas (8) taking into account the relationship (13) between the Mach numbers M_- and M_+. These equations allow to construct domains of existence (Figure 5).

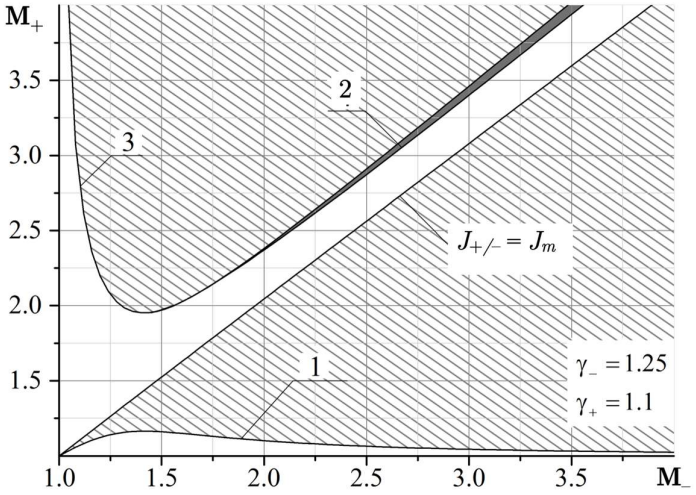

Figure 5. The domains of existence of characteristic refraction at the interface between the hot hydrocarbon fuel mixture ($\gamma = 1.1$) and the products of its combustion ($\gamma = 1.25$), where domains 1, 2 and 3 are the first, second and third roots of equation (8).

Figure 6 shows the dependence of the intensity of the incident shock wave corresponding to the characteristic refraction. It is seen that there are solutions with one and two roots of equation (8). The three roots are not physically realized.

Preprints (www.preprints.org) | NOT PEER-REVIEWED | Posted: 22 June 2021 doi:10.20944/preprints202106.0546.v1

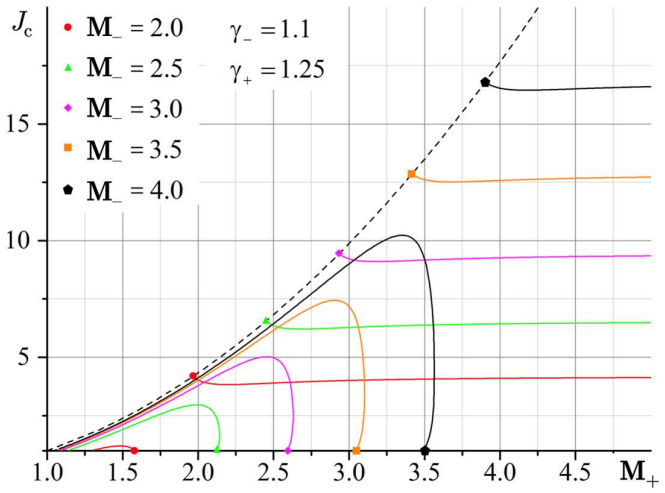

Figure 6. Dependence of the intensity J_c of the incident shock corresponding to the characteristic refraction on the Mach numbers M- and M+ in flows separated by a tangential discontinuity. The dotted line shows the dependencies corresponding to the case when the refracted shock has the maximum intensity $J_2 = J_m$.

4. Domains of existence

If the intensity of the incident shock is $J_1 \neq J_c$, then it passes the tangential discontinuity with partial reflection. Depending on the intensity of the tangential discontinuity J_τ, the reflected discontinuity r_3 can be either a compression shock σ_3 or a rarefaction wave ω_3. If r_3 is a shock wave, then at certain intensities J_1 of the incident shock, the solution of equation (5) may be not existent, since polar (3) emitted from point (1) corresponding to J_1 does not intersect with polar (1) (Figure 7). The shock-wave structure corresponding to MRef is shown in Figure 8.

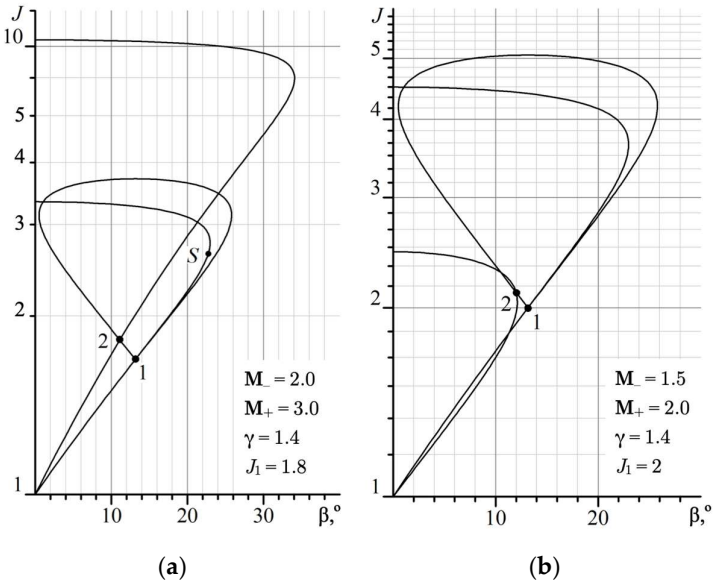

Figure 7. Regular refraction when the flow behind the reflected flow is supersonic (a) and subsonic (b).

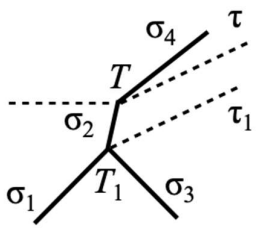

Figure 8. Shock wave configuration for Mach refraction.

For irregular refraction, the incident shock σ_1 branches with the formation of a reflected shock σ_3 and a main shock σ_2 (the Mach stem). The main shock experiences characteristic refraction on the tangential discontinuity τ. The Mach stem is enclosed between two points T and T_1, from which tangential discontinuities originate, τ and τ_1. Figure 9 shows the regions of existence of a shock-wave structure with a different type of reflected discontinuity r_3 (Figure 1), which are formed during refraction of the shock σ_1 at the tangential discontinuity τ.

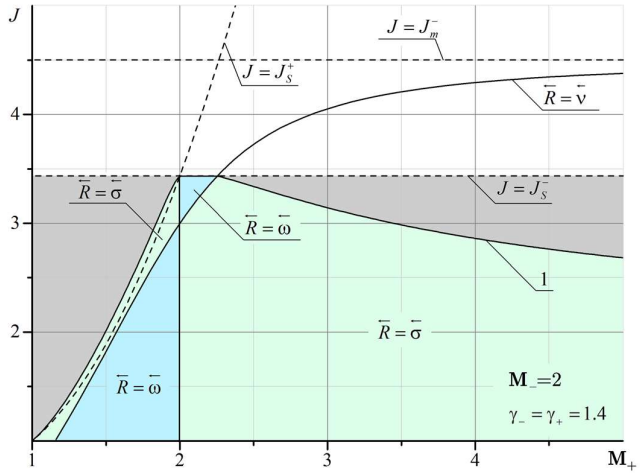

Figure 9. Domains of existence of various types of hydrocarbons formed during refraction of a shock with intensity J propagating from a flow with a Mach number $M_-=2$ into a flow with a Mach number M_+. The grey area corresponds to irregular refraction with a supersonic flow $M_1>1$ behind a shock σ_1, and white area corresponds to irregular refraction with a subsonic flow behind a shock σ_1.

It can be seen that at $M_-=2$ and $M_+<2$, there are quite extensive regions with both the reflected shock wave σ_3 and the reflected rarefaction wave ω_3. As M_- increases, the domains of existence of the reflected σ_3 at $M_+<M_-$ are significantly reduced (Figures 10 and 11).

Preprints (www.preprints.org) | NOT PEER-REVIEWED | Posted: 22 June 2021 doi:10.20944/preprints202106.0546.v1

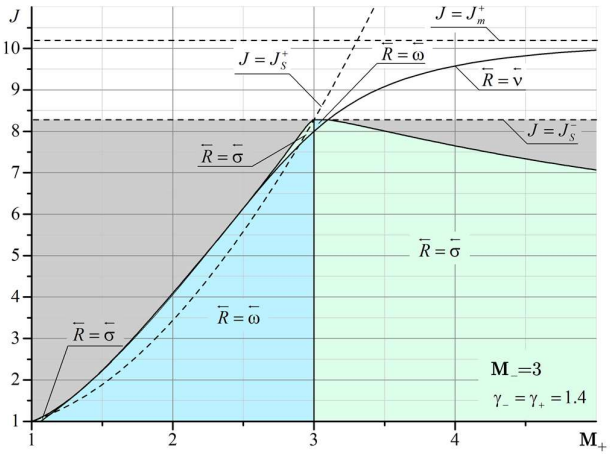

Figure 10. Domains of existence of various types of hydrocarbons formed during refraction of a shock with intensity *J*, propagating from a flow with a Mach number M-=3 into a flow with a Mach number M+.

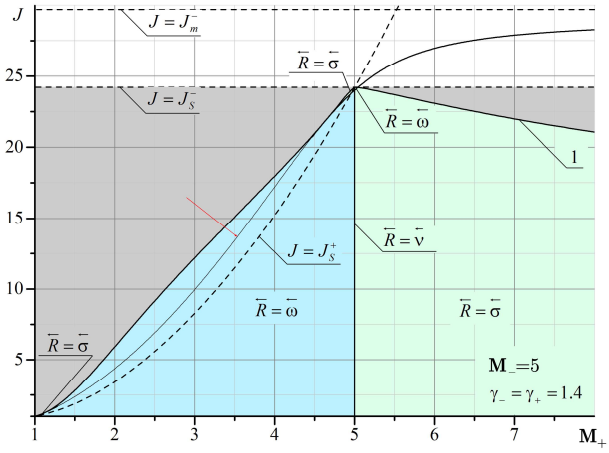

Figure 11. Domains of existence of various types of hydrocarbons formed during refraction of a shock with intensity *J*, propagating from a flow with a Mach number of M-=5 to a flow with a Mach number of M+.

The boundary of irregular refraction with supersonic flow behind the shock σ_1 (gray area in Figures 9-11) is bounded from above by the intensity of the incoming shock $J = J_s$. It should also be noted that the line corresponding to the characteristic refraction at $M_+<M_-$ gradually shifts to the left and goes into the MRef region. This is especially noticeable in Figure 11. The red arrow shows a thin line corresponding to the solution in the plane of the shock polar in Figure 12. This line marks the characteristic refraction.

 doi:10.20944/preprints202106.0546.v1

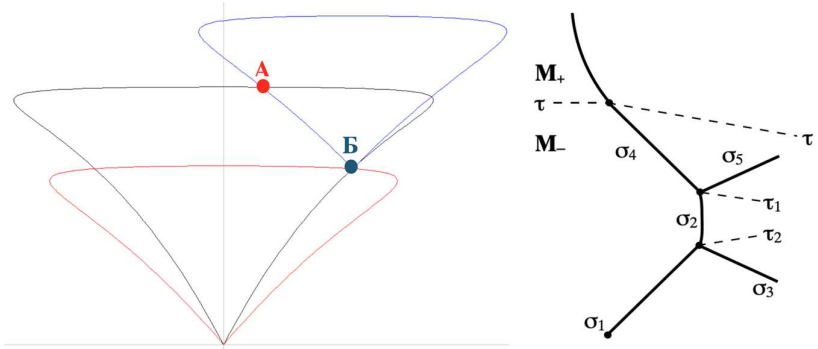

(**a**) (**b**)

Figure 12. Ambiguity of the solution on the polar plane: irregular refraction (A), characteristic refraction (B): (a) solutions on the plane of shock polar, (b) shock-wave structure corresponding to the Mach refraction MRef.

In the area enclosed between the solid line separating the gray and blue areas and the thin line, the solutions are ambiguous. One solution (point B in Figure 12a) corresponds to characteristic refraction, the other solution (point A in Figure 12b) corresponds to MRef with shock-wave structure shown in Figure 12b. The flow above τ behind the refracted shock σ_4 is subsonic. Between these two lines lies a region with a reflected rarefaction wave. Consequently, depending on the initial conditions, either RRef with a reflected wave or MRef with a shock-wave structure can be realized as shown in Figure 12b.

Figures A1–A17presented in Appendix A show the domains of existence of MRef and RRef refractions with different types of reflected discontinuities, where $\bar{R} = \bar{\nu}$ is the line of characteristic refraction, $\bar{R} = \bar{\omega}$ is RRef with reflected wave, $\bar{R} = \bar{\sigma}$ is with a reflected shock.

4. Conclusions

The refraction of an oblique shock wave on a tangential discontinuity is considered. The domains of existence of shock-wave structures with reflected discontinuities of two types are constructed, the rarefaction wave and the shock wave, and the characteristic refraction separating these two cases. It is shown that for characteristic refraction there are parameter regions with one and two solutions. Conditions for the existence of regular and Mach refraction are formulated, boundaries separating them are constructed for various gases.

Author Contributions: Conceptualization, P.Bulat and V.Upyrev; methodology, P.Bulat; software, V.Upyrev and A.Melnikova; validation, A.Melnikova and K.Volkov; formal analysis, P.Bulat; investigation, V.Upyrev; resources, K.Volkov; writing-original draft preparation, P.Bulat; writing-review and editing, A.Melnikova and K.Volkov; visualization, V.Upyrev; supervision, P.Bulat. All authors have read and agreed to the published version of the manuscript.

Funding: This work was financially supported by the Ministry of Science and Higher Education of Russian Federation during the implementation of the project "Creating a leading scientific and technical reserve in the development of advanced technologies for small gas turbine, rocket and combined engines of ultra-light launch vehicles, small spacecraft and unmanned aerial vehicles that provide priority positions for Russian companies in emerging global markets of the future", No. FZWF-2020-0015.

Conflicts of Interest: The authors declare no conflict of interest.

 doi:10.20944/preprints202106.0546.v1

Appendix A

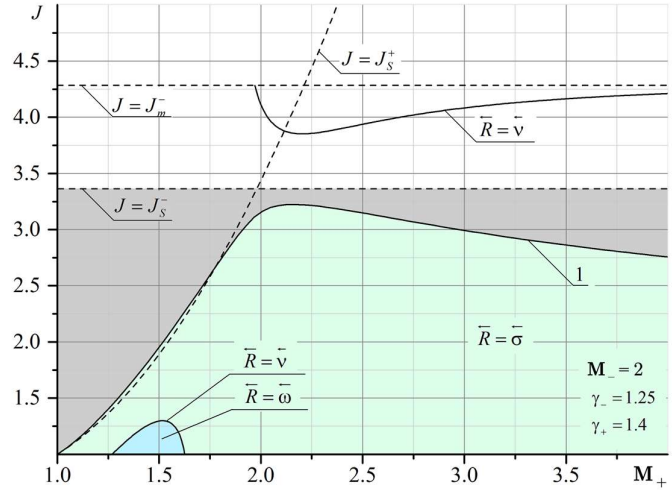

Figure A1. Domains of existence of reflected discontinuities for refraction from a gas consisting of combustion products into a diatomic gas. The Mach number of the flow from which the shock comes is M_=2.

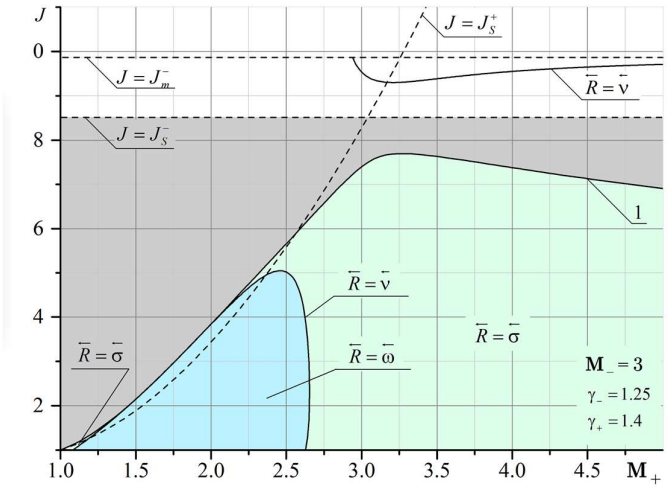

Figure A2. Domains of existence of reflected discontinuities for refraction from a gas consisting of combustion products into a diatomic gas. The Mach number of the flow from which the shock comes is M_=3.

Preprints (www.preprints.org) | NOT PEER-REVIEWED | Posted: 22 June 2021 doi:10.20944/preprints202106.0546.v1

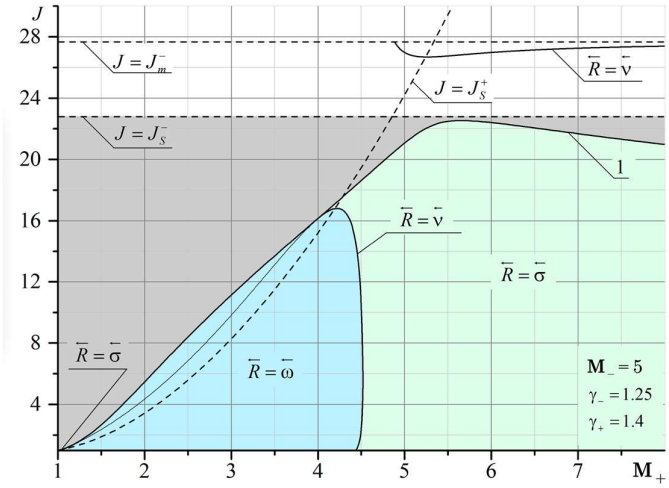

Figure A3. Domains of existence of reflected discontinuities for refraction from a gas consisting of combustion products into a diatomic gas. The Mach number of the flow from which the shock comes is M_=5.

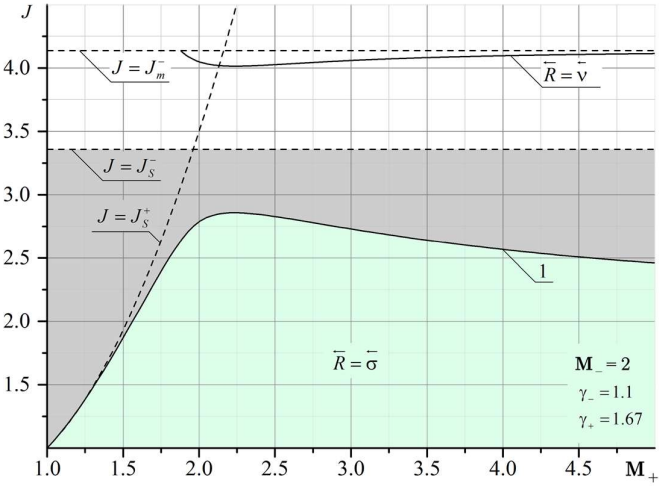

Figure A4. Domains of existence of reflected discontinuities for refraction from a gas consisting of combustion products into a monatomic gas. The Mach number of the flow from which the shock comes is M_=2.

Preprints (www.preprints.org) | NOT PEER-REVIEWED | Posted: 22 June 2021 doi:10.20944/preprints202106.0546.v1

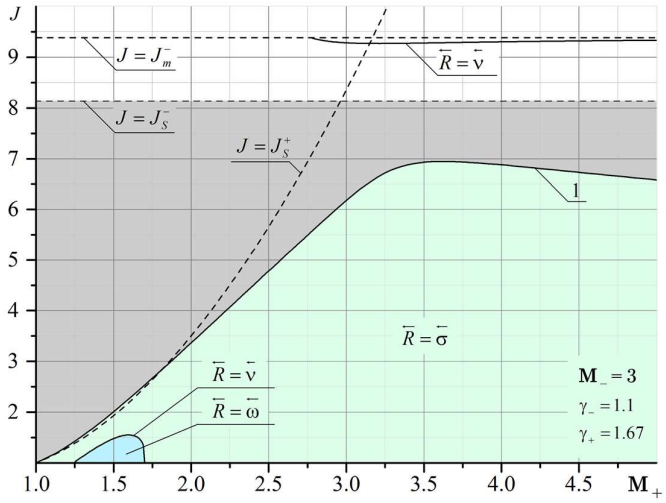

Figure A5. Domains of existence of reflected discontinuities for refraction from a gas consisting of combustion products into a monatomic gas. The Mach number of the flow from which the shock comes is M_=3.

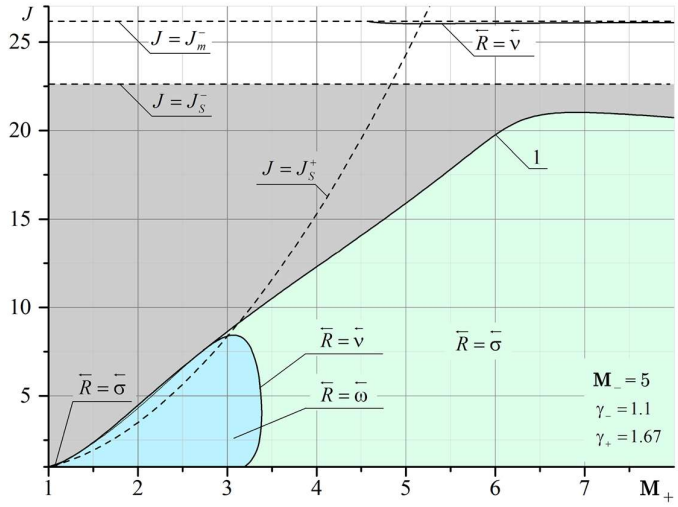

Figure A6. Domains of existence of reflected discontinuities for refraction from a gas consisting of combustion products into a monatomic gas. The Mach number of the flow from which the shock comes is M_=5.

Preprints (www.preprints.org) | NOT PEER-REVIEWED | Posted: 22 June 2021 doi:10.20944/preprints202106.0546.v1

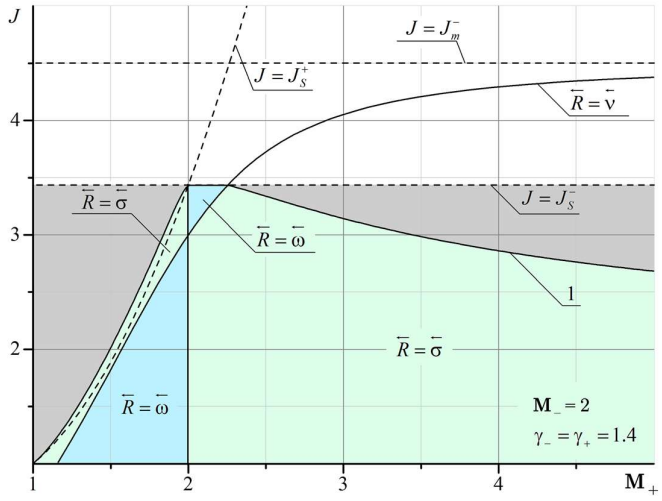

Figure A7. Domains of existence of reflected discontinuities for refraction in a flow of diatomic gas. The Mach number of the flow from which the shock comes is M_=2.

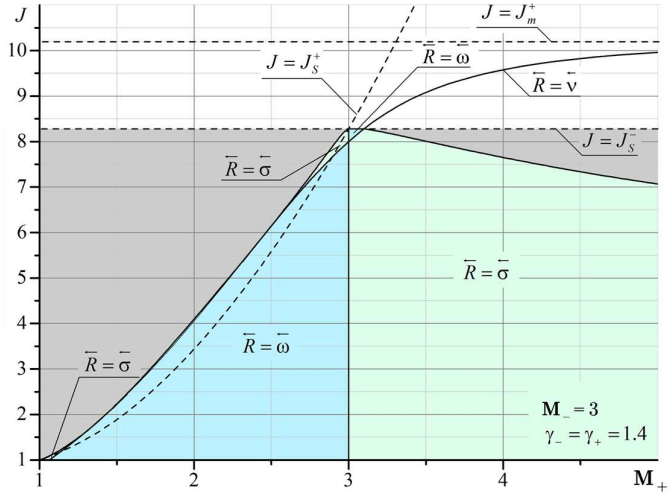

Figure A8. Domains of existence of reflected discontinuities for refraction in a flow of diatomic gas. The Mach number of the flow from which the shock comes is M_=3.

Preprints (www.preprints.org) | NOT PEER-REVIEWED | Posted: 22 June 2021 doi:10.20944/preprints202106.0546.v1

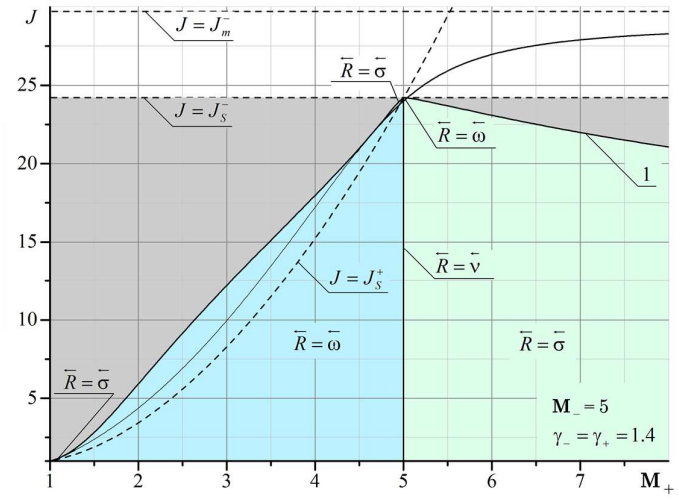

Figure A9. Domains of existence of reflected discontinuities for refraction in a flow of diatomic gas. The Mach number of the flow from which the shock comes is M_=5.

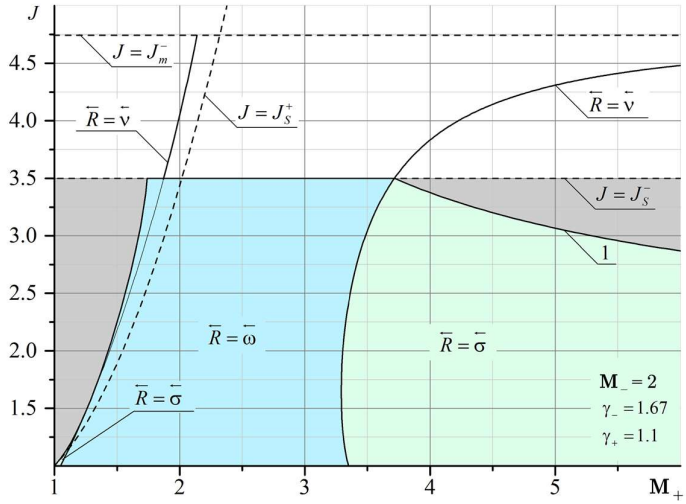

Figure A10. Domains of existence of reflected discontinuities for refraction from a monatomic gas into a gas consisting of combustion products. The Mach number of the flow from which the shock comes is M_=2.

Preprints (www.preprints.org) | NOT PEER-REVIEWED | Posted: 22 June 2021 doi:10.20944/preprints202106.0546.v1

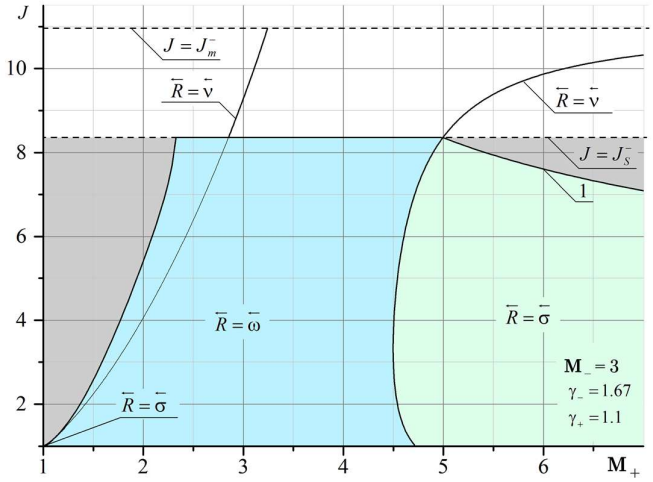

Figure A11. Domains of existence of reflected discontinuities for refraction from a monatomic gas into a gas consisting of combustion products. The Mach number of the flow from which the shock comes is M_=3.

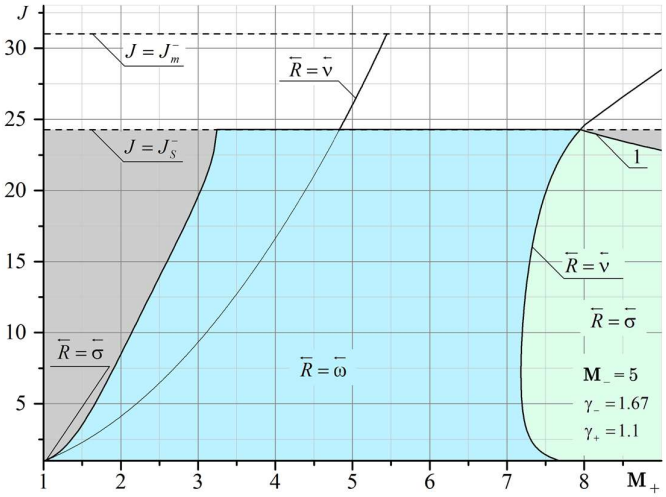

Figure A12. Domains of existence of reflected discontinuities for refraction from a monatomic gas into a gas consisting of combustion products. The Mach number of the flow from which the shock comes is M_=5.

Preprints (www.preprints.org) | NOT PEER-REVIEWED | Posted: 22 June 2021 doi:10.20944/preprints202106.0546.v1

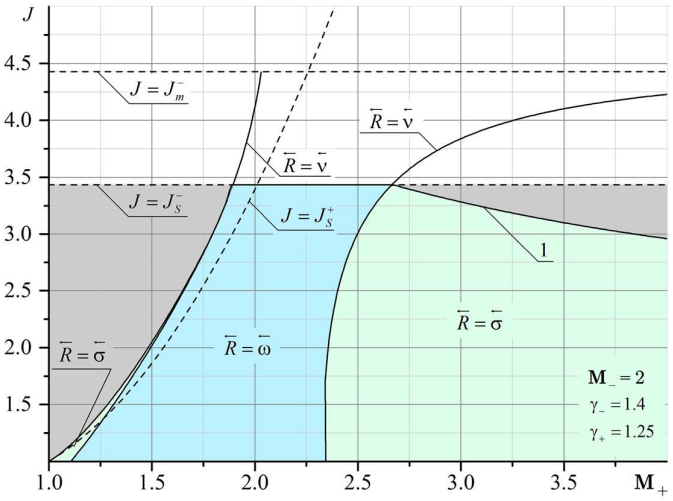

Figure A13. Domains of existence of reflected discontinuities for refraction from a diatomic gas into a gas consisting of combustion products. The Mach number of the flow from which the shock comes is M_=2.

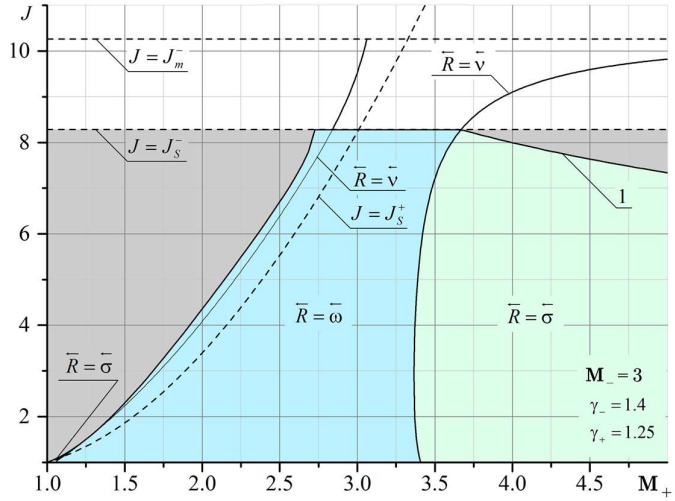

Figure A14. Domains of existence of reflected discontinuities for refraction from a diatomic gas into a gas consisting of combustion products. The Mach number of the flow from which the shock comes is M_=3.

 doi:10.20944/preprints202106.0546.v1

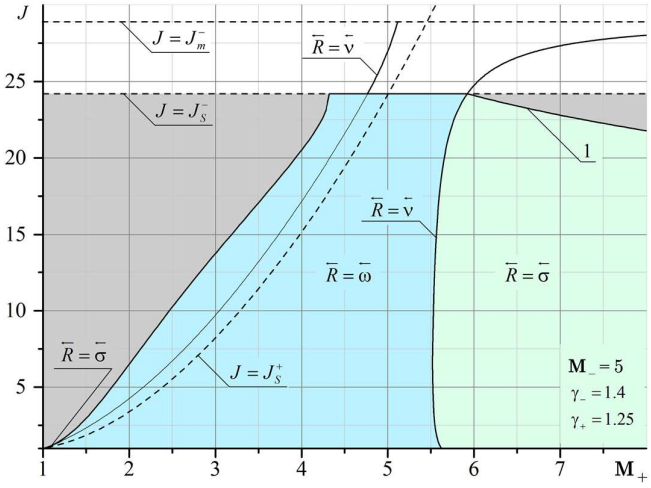

Figure A15. Domains of existence of reflected discontinuities for refraction from a diatomic gas into a gas consisting of combustion products. The Mach number of the flow from which the shock comes is M_=5.

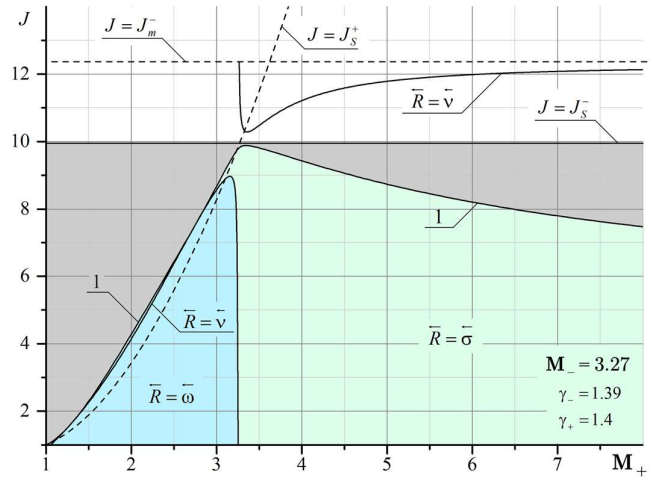

Figure A16. Domains of existence of reflected discontinuities for refraction from a hydrogen/oxygen mixture at Mach number M_=3.27 corresponding to Chapman-Judge detonation.

 doi:10.20944/preprints202106.0546.v1

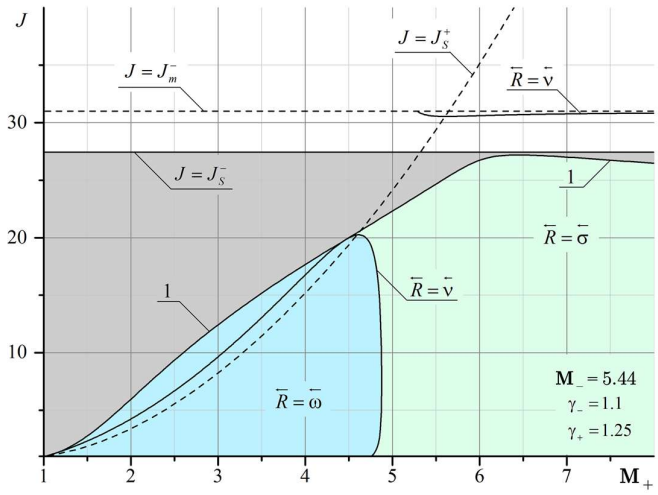

Figure A17. Domains of existence of reflected discontinuities for refraction from a propane/air/combustion products mixture at Mach number M_=5.46 corresponding to Chapman-Judge detonation.

References

1. Adrianov, A.L.; Starykh, A.L.; Uskov, V.N. *Interference of steady gas dynamic discontinuities*. Nauka: Novosibirsk, Russia, 1995.
2. Jahn, R.G. The refraction of shock waves at a gaseous interface. *Journal of Fluid Mechanics* **1956**, *1*, 457–489.
3. Zeng, S.; Takayama, K. On the refraction of shock wave over a slow-fast gas interface. *Acta Astronautica* **1996**, *38*, 829–838.
4. Starykh, A.L. Irregular interaction of shock waves between themselves and tangential discontinuities. *Numerical Methods in Continuum Mechanics* **1986**, *.7*, 119–124.
5. Uskov, V.N. Interference of gas dynamics and tangential discontinuities. *Fluids Dynamics* **1979**, *4*, 191–197.
6. Abd-El-Fattah, A.M.; Henderson, L.F. Shock waves at a fast-slow gas interface. *Journal of Fluid Mechanics* **1978**, 86, 15–32.
7. Abd-El-Fattah, A.M.; Henderson, L.F. Shock waves at a slow-fast gas interface. *Journal of Fluid Mechanics* **1978**, *89*, 79–95.
8. Henderson, L.F.; Colella, P.; Puckett, E.G. On the refraction of shock waves at a slow-fast gas interface. *Journal of Fluid Mechanics* **1991**, *224*, 1–27.
9. Uskov, V.N.; Starykh, A.L. Analysis of the region of existence of stationary gasdynamic discontinuities equation solution. *Unsteady gas flows with shock waves* **1990**, 359–372.
10. Nouragliev, R.R.; Sushchikh, S.Y.; Dinh, T.N.; Theofanous, T.G. Shock wave refraction patterns at interfaces. *International Journal of Multiphase Flow* **2005**, *31*, 969–995.
11. Henderson, L.F. On the refraction of shock waves. Journal of Fluid Mechanics **1989**, 198, 365–386.
12. Samtaney, R.; Zabusky, N.J. On shock polar analysis and analytical expressions for vorticity deposition in shock-accelerated density stratified interfaces. *Physics of Fluids* **1993**, *5*, 1285–1287.
13. Samtaney, R.; Pullin, D.I. On initial-value and self-similar solutions of the compressible Euler equations. *Physics of Fluids* **1996**, *8*, 2650–2655.
14. Samtaney, R. Suppression of the Richtmyer–Meshkov instability in the presence of a magnetic field. *Physics of Fluids* **2003**, *15*, L53–L56.
15. Wheatley, V.; Pullin, D.I.; Samtaney, R. Regular shock refraction at an oblique planar density interface in magnetohydrodynamics. *Journal of Fluid Mechanics* **2005**, *522*, 179–214.
16. Yang, X.; Chern, I.; Zabusky, N.J.; Samtaney, R.; Hawley, J.F. Vorticity generation and evolution in shock-accelerated density-stratified interfaces. *Physics of Fluids* **1992**, *4*, 1531–1540.
17. Delmont, P.; Keppens, R.; van der Holst, B. An exact Riemann solver based solution for regular shock refraction. *Journal of Fluid Mechanics* **2009**, *627*, 33–53.
18. Pember, R.B.; Anderson, R.W. Comparison of direct Eulerian Godunov and Lagrange plus remap, artificial viscosity schemes. *AIAA Paper* **2001**, *2001-2644*.
19. Samtaney, R.; Meiron, D.I. Hypervelocity Richtmyer–Meshkov instability. *Physics of Fluids* **1997,** *9*, 1783–1803.
20. Banuti, D.T.; Grabe, M.; Hannemann, K. Steady shock refraction in hypersonic ramp flow. *AIAA Paper* **2011**, *2011-2215*.
21. Brouillette, M. The Richtmyer–Meshkov instability. *Annual Review of Fluid Mechanics* **2002,** *34*, 445–468.
22. Dutta, S.; Glimm, J.; Grove, J.W.; Sharp, D.H.; Zhang, Y. Error comparison in tracked and untracked spherical simulations. *Computers and Mathematics with Applications* **2004**, *48*, 1733–1747.
23. Liu, T.C.; Khoo, B.C.; Yeo, K.S. The simulation of compressible multi-medium flow. I. A new methodology with test applications to 1D gas–gas and gas–water cases. *Computers and Fluids* **2001**, *30*, 291–314.

24. Liu, T.C.; Khoo, B.C.; Yeo, K.S. The simulation of compressible multi-medium flow. II. Applications to 2D underwater shock refraction. *Computers and Fluids* **2001,** 30, 315–337.
25. Silnikov, M.V.; Chernyshov, M.V.; Uskov, V.N. Analytical solutions for Prandtl-Meyer wave – oblique shock overtaking interaction. Acta Astronautica 2014, 99, 175–183.
26. Shoev, G.V.; Ivanov, M.S. Numerical study of shock wave interaction in steady flows of a viscous heat-conducting gas with a low ratio of specific heats. *Thermophysics and Aeromechanics* **2016**, *23*, 343–364.
27. Gounko, Y.P. Patterns of steady axisymmetric supersonic compression flows with a Mach disk. *Shock Waves* **2017**, *27*, 495–506.
28. Vasilev, E.I. The nature of the triple point singularity in the case of stationary reflection of weak shock waves. *Fluid Dynamics* **2016**, *51*, 804–813.
29. Bao, C.-Y.; Wu, Z.-N. Size and shape of shock waves and slipline for Mach reflection in steady flow. *Journal of Fluid Mechanics* **2017**, *818*, 116–140.
30. Roy, S.; Gopalapillai, R. An analytical model for asymmetric Mach reflection configuration in steady flows. *Journal of Fluid Mechanics* **2019**, *863*, 242–268.
31. Lin, L.; Bao, C.-Y.; Wum Z.N. Study of asymmetrical shock wave reflection in steady supersonic flow. *Journal of Fluid Mechanics* **2019**, *864*, 848–875.
32. Chernyshov, M.V.; Murzina, K.E.; Matveev, S.A.; Yakovlev, V.V. Shock-wave structures of prospective combined ramjet engine. *IOP Conference Series: Materials Science and Engineering* **2019**, *618*, 012068.
33. Alekseeva, M.M.; Matveev, S.A.; Savelova, K.E.; Chernyshov M.V. Interaction of steady gas-dynamic discontinuities and waves on supersonic gas jet flows from rocket engines. *AIP Conference Proceedings* **2021**, *2318*, 06000.